Front. Optoelectron. 2017, 10(3): 255–266
DOI 10.1007/s12200-017-0717-5

REVIEW ARTICLE

In vivo skin imaging prototypes "made in Latvia"

Janis SPIGULIS (✉)

Biophotonics Laboratory, Institute of Atomic Physics and Spectroscopy, University of Latvia, Riga, LV-1586, Latvia

Abstract This paper briefly reviews the operational principles and designs of portable *in vivo* skin imaging prototypes developed at the Biophotonics Laboratory of the Institute of Atomic Physics and Spectroscopy, University of Latvia. Four types of imaging devices are presented. Multi-spectral imagers ensure distant mapping of specific skin parameters (e.g., distribution of skin chromophores). Autofluorescence photobleaching rate imagers show potential for skin tumor assessment and margin delineation. Photoplethysmography video-imagers remotely detect cutaneous blood pulsations and provide real-time information on the human cardiovascular state. Multimodal skin imagers perform the above-mentioned functions by acquiring several spectral and video images using the same image sensor.

Keywords multispectral skin imaging, autofluorescence photobleaching, remote photoplethysmography

1 Introduction

Biomedical imaging has become a powerful tool for diagnostics and monitoring human health. Apart from routine clinical imaging modalities such as X-ray, ultrasound, endoscopy, computed tomography, and magnetic resonance imaging, several advanced "open air" optical tissue imaging methods and technologies have been introduced recently. Their main advantages are remote operation (which helps to avoid infections) and non-invasiveness (leaving the treated tissue's structure intact). In addition, digital imaging enables quantitative documentation of the tissue condition and changes in the tissue condition following specific interactions.

This paper briefly presents the operational principles and designs of portable *in vivo* skin imaging prototypes that have been developed since the previous review [1] at the Biophotonics Laboratory of the Institute of Atomic Physics and Spectroscopy, University of Latvia. Four types of imaging devices are presented. Multi-spectral imagers offer possibilities for distant mapping of specific skin parameters (e.g., distribution of skin chromophores, cutaneous blood oxygen saturation, erythema index), facilitating better diagnostics of skin malformations. Autofluorescence photobleaching rate imagers show a promising potential for skin tumor identification and margin delineation. Photoplethysmography video-imagers enable remote detection of cutaneous blood pulsations and can provide real-time information on cardiovascular parameters and anesthesia efficiency. Finally, multimodal skin imagers perform several of the above-mentioned functions by acquiring several spectral and video images using the same image sensor.

Received March 30, 2017; accepted May 26, 2017

E-mail: janis.spigulis@lu.lv

2 Prototypes

2.1 Prototype devices for multispectral skin imaging

Multispectral imaging is based on the acquisition of a limited number (typically 3 to 10) of images within relatively narrow non-overlapping spectral bands [2]. The captured spectral images of skin can be further converted into parametric images, e.g., two-dimensional (2D) maps of the distributions of skin melanin and hemoglobin concentration [3,4]. In the visible spectral range, a relatively simple 3-chromophore skin model can be applied for obtaining chromophore distribution maps over the imaged area [5]. The hardware implementing this approach should ensure easy and fast acquisition of three narrowband spectral images of skin. One way to achieve this is using subsequent narrowband illumination by means of different-color light emitting diodes (LEDs), and by capturing one spectral image for each illumination mode [3]. This approach was examined earlier using a compact research grade system comprising red-green-blue (RGB) camera and LED illumination ring [6]. As the next

steps, three prototype devices comprising commercial consumer cameras and spectrally specific illuminators were developed.

2.1.1 RGB-LED smartphone add-on illumination system

Owing to the rapid development of communication technologies, a number of smartphone camera-based health assessment software applications have become available, working both in ambient light and under white LED illumination of the same phone [7–9]. Such applications may provide, for instance, information about malignancy of skin lesions [9]. To extend the smartphone applications for skin evaluation, we developed a technique for mapping main skin chromophores using an RGB light source that was specially designed as an add-on for various smartphone models.

The system is schematically presented in Fig. 1. A smartphone is fixed on a flat sticky surface with a window for its rear camera [10], which is surrounded from the bottom by a ring of LEDs mounted within a cylindrical screening spacer (6 cm between the skin and camera). The ring includes four types of LEDs, with four diodes of each type: white – to find and adjust the location of the skin malformation, and colored – with emission in blue (maximum at 460 nm), green (maximum at 535 nm), and red (maximum at 663 nm) spectral bands (Fig. 1(b)), which are suitable for mapping three skin chromophores. LEDs are operated in the continuous mode and are switched on and off manually or automatically by dedicated software that uses a *bluetooth* connection between the smartphone and the illumination system. Illumination and image detection are performed normally to the skin surface. Two orthogonally oriented polarizers are used in front of the LEDs and smartphone camera, respectively, to reduce the detection of skin specular reflection. Five AA 2800 mAh rechargeable battery blocks constitute the power supply of the system.

Figure 2(a) shows more design details of the prototype. A driver placed in compartment 10 ensures a *bluetooth* wireless connection between the smartphone and the illumination unit and enables automatic sequential on-off switching of the color LEDs within less than 1 s (capturing one image per illumination) by command from the smartphone's touchscreen. Using specially developed software, the obtained spectral images are further transmitted via a mobile network to a remote server where they are converted into three chromophore (melanin, oxy- and deoxy-hemoglobin) distribution maps that are then transmitted back and displayed on the smartphone's touchscreen.

The RGB-LED prototype device and its validation are described in detail in Ref. [11].

2.1.2 Modified multispectral video-microscope

A number of digital microscopes are small hand-held devices that can be connected to a personal computer (PC) using a universal serial bus (USB) cable; these devices can be also used for visual skin assessment [12]. A typical digital microscope consists of a webcam with a high-power macro-lens and a built-in LED as a light source. The advantages of such microscopes are their compactness, low power consumption and relatively low price, typically a few hundreds of USD. Most digital microscopes have white illumination source(s) and some of them also have ultraviolet (UV) illuminators [13]. These devices, however, cannot be used for detailed spectral analysis of skin. To overcome this drawback, we adapted a standard digital microscope (model *DinoLite* AD413, series AM-4013) for multispectral imaging by replacing the built-in LEDs with specifically selected color LEDs and by developing the LED management software.

Figure 3 shows the block diagram of our custom-modified microscope. A standard white/UV LED illuminator ring is replaced by a laboratory-designed illuminator ring comprising 16 LEDs combined in four groups: 1) four infrared (IR) 940-nm-wavelength LEDs, 2) four red 660-nm-wavelength LEDs, 3) four green 545-nm-wavelength LEDs, and 4) four blue 450-nm-wavelength LEDs. Each group of LEDs receives a current of 80 mA that is fed by LED drivers that are controlled by a FTDI USB controller.

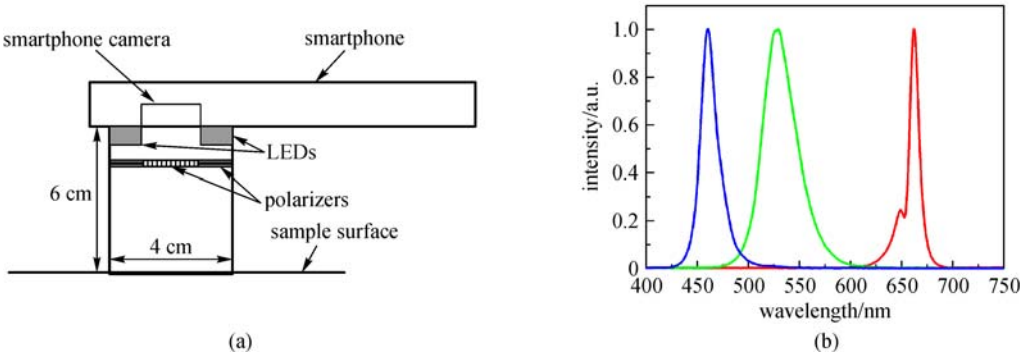

Fig. 1 Design scheme of the smartphone RGB illuminator (a), and normalized emission spectra of the used color LEDs

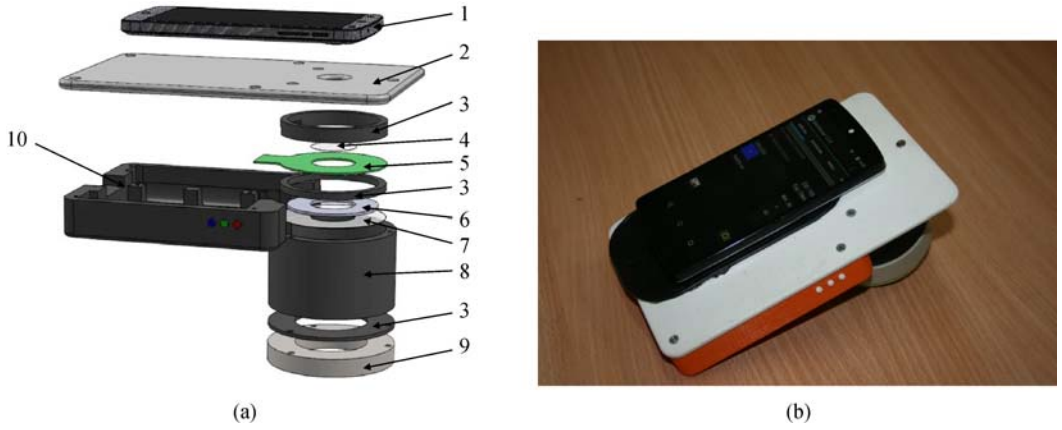

Fig. 2 Design details of the smartphone-LED prototype device (a) and its outlook with a smartphone on it (b). 1 – smartphone, 2 – sticky fixing platform with a camera window, 3 – holding ring, 4 – polarizer of the detected light, 5 – LED ring comprising four sets of LEDs, 6 – light diffuser, 7 – illumination polarizer (oriented orthogonally to the polarizer 4), 8- screening spacer, 9 – silicone skin contact ring, 10 – compartment for batteries and electronic components

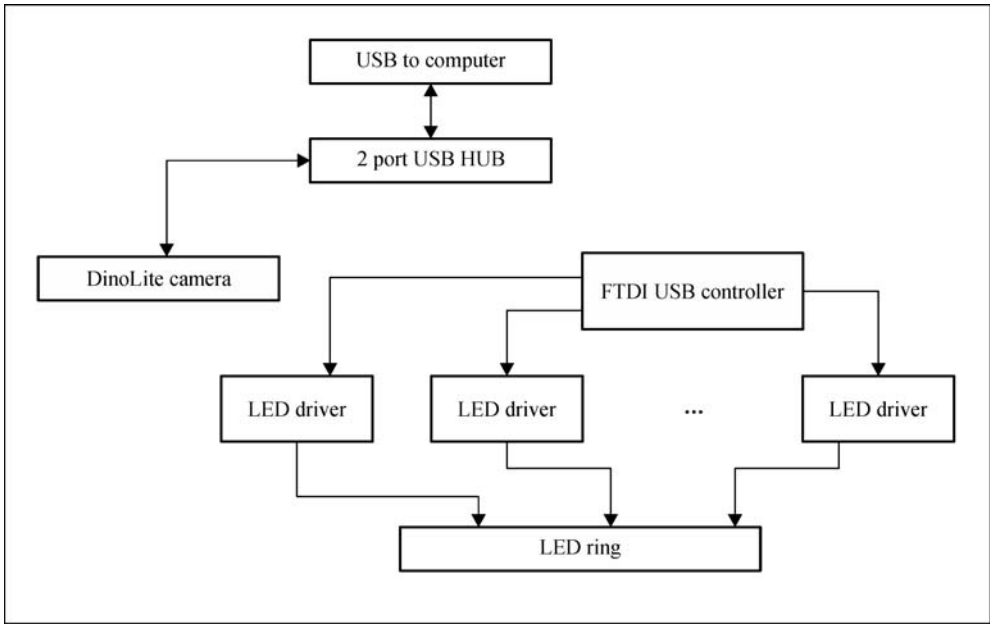

Fig. 3 Block diagram of the modified video-microscope

The two-port USB hub provides control over the LEDs and the complementary metal-oxide semiconductor (CMOS) image sensor of the microscope. The delivery of power, the switching of LEDs, and the CMOS control are accomplished via the USB interface.

The custom-designed control unit module is installed on the rear side of the microscope, as shown on Fig. 4(a). The laboratory-made 16-LED ring is mounted on the front side (Fig. 4(b)); it is even more compact than the original 8-LED *DinoLite* ring. For better homogeneity of skin illumination, a diffuser is attached to the new LED-ring. To avoid detection of the directly reflected radiation from the skin surface (thus distinguishing the diffusely reflected radiation from the upper layers of skin), a pair of orthogonally oriented polarizing filters is added: one of them directly after the diffuser, and the other, in front of the camera sensor matrix.

The microscope is computer-controlled. The custom-developed program written in MatLab with a standard FTDI USB driver and a custom LED driver (written in the C programming language) controls the LEDs and the acquisition of images. The software provides two image-processing modes: 1) the preview mode, for focusing the microscope on the skin object, and 2) the video acquisition/processing mode, in which the software sequentially switches on-off the LEDs and triggers the video sensor. In each measurement, four frames are captured (taken within the four wavelength bands). After recording, the

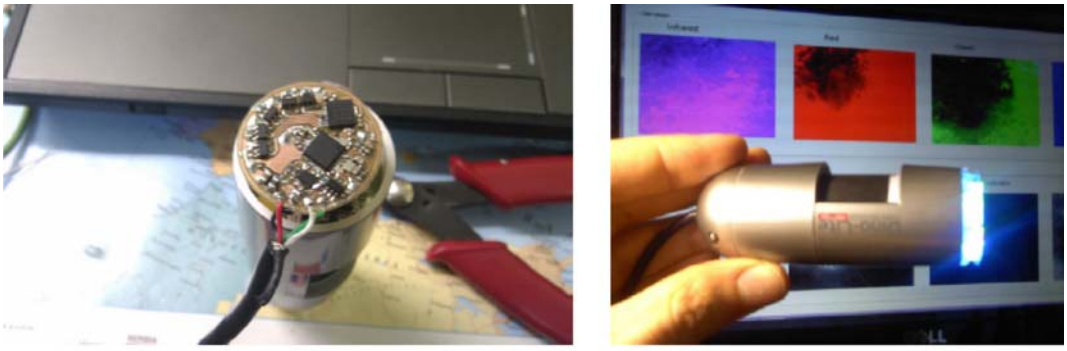

Fig. 4 Developed LED control unit (a), and the modified video-microscope with the replaced illumination unit (b)

images are stored in a 4-image matrix and saved as a data file for further processing. The image-processing software allows to calculate the distribution maps of three above-mentioned skin chromophores, erythema index, and melanoma/nevus differentiation parameter [14].

A detailed description of the modified video-microscope and its validation can be found in Refs. [15–17].

2.1.3 Prototypes for smartphone-mediated express mapping of skin chromophores at multi-laser illumination

If skin is evenly illuminated by several laser sources, monochromatic spectral images can be extracted from a single RGB image file [18], making it possible to map several chromophores in one snapshot. Such approach expedites image processing and excludes image artifacts caused by tissue movements. The first demonstration of skin hemoglobin snapshot RGB mapping at double-wavelength laser illumination was reported in Ref. [19]. Later, mapping of three main skin chromophores at triple-wavelength laser illumination was demonstrated with laboratory-made [20] and smartphone-based [21] setups.

The general concept of snapshot skin chromophore mapping at fixed wavelengths is illustrated at Fig. 5. Let us suppose that an RGB color image of skin is acquired under illumination that comprises only three equal intensity spectral lines, corresponding to wavelengths λ_1, λ_2, and λ_3 (vertical lines in Fig. 5). With respect to the spectral sensitivity of the RGB image sensor and the cross-talk between its detection bands at the particular wavelengths, three monochromatic spectral images can be extracted from the color image data set using the technique described in Refs. [18,24]. If the skin surface reflection is suppressed (e.g., using crossed polarizers), variations in the chromophore composition lead to changes in the intensities of diffusely reflected light, at each of the fixed wavelengths. Such variations in the pathology region relative to the healthy skin can be estimated by measuring the intensities of reflected light from equally sized regions of interest in the pathology (I_j) and the adjacent healthy skin (I_{oj}). The ratios I_j/I_{oj} for each pixel or pixel's group of three monochromatic spectral images contain information about changes in the concentrations of the three chromophores, which can be further mapped over the entire image area [21].

A compact smartphone-compatible three-wavelength illuminator has been designed, assembled, and tested in

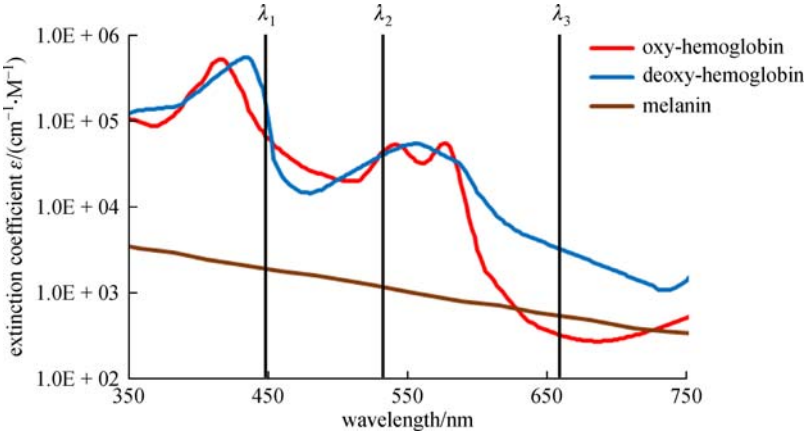

Fig. 5 Absorption of three main skin chromophores [22,23] at three fixed wavelengths

the laboratory and clinic. The illumination unit comprises six laser modules, an optical element for laser beam management and an electronics compartment. Figure 6 shows the design details (Fig. 6(a)) and the outlook of the operating prototype with a smartphone on it (Fig. 6(b)). To ensure uniform three-wavelength illumination of the round target area, an optical element with a flat ring-shaped laser diffuser was developed [10]. The illumination wavelengths (448, 532, and 659 nm) were emitted by three pairs of compact 20-mW-power laser modules (models *PGL-DF-450 nm-20 mW-15011564, PGL-VI-1-532 nm-20 mW-15030443* and *PGL-DF-655 nm-20 mW-150302232*, Changchun New Industries Optoelectronics Tech. Co., Ltd.).

Laser modules (1, Fig. 6(a) – 3 out of 6 are shown) of each equal-wavelength pair were mounted at the opposite sides on the internal wall of a hollow 3D-printed plastic shielding cylinder 2; the round bottom opening of this cylinder (diameter, 40 mm) was in contact with skin and formed the field of view for the smartphone camera, positioned 80 mm away. All six coaxial laser beams were pointed to the 45° conical reflecting edge of a transparent disc 3 (beam collector) made of standard Plexiglas; after reflections, the beams converged in the radial direction toward an internal ring-shaped flat milky-Plexiglas diffuser 4. The upper and side surfaces of the collector/diffuser unit were mirrored by a vacuum-sputtered Al-coating. As a result, the flat diffuser 4 evenly illuminated the 65 mm^2 distant skin target area simultaneously by three laser wavelengths. The smartphone – model *Google Nexus 5,* 8Mpx image sensor *SONY IMX179* with known RGB sensitivities – was placed on a flat sticky platform 5 (Fig. 6 (a)) with a round window for the smartphone's rear camera, co-aligned with the internal opening of the diffuser 4. The round camera window was covered by a film polarizer; another film with orthogonal polarization axis covered the diffuser 4 from the bottom, thus avoiding detection of skin surface-reflected light by the smartphone's camera. The estimated spatial resolution of the imaging system was better than 0.1 mm.

The single-snapshot RGB technique is not applicable for express-mapping of more than three chromophores. The double-snapshot approach [25] for obtaining four monochromatic images has been implemented in a model device comprising a switchable four-laser-wavelengths illuminator and a smartphone. Figure 7 shows the design scheme and the outlook of a smartphone add-on illuminator intended for mapping of four skin chromophores, e.g., melanin, oxy-hemoglobin, deoxy-hemoglobin and bilirubin. Two of the laser modules can be manually switched on and off, providing two sets of three-laser-wavelengths illuminations (405, 532, and 650 nm; 450, 532, and 650 nm). Four rechargeable AA-type batteries are used for power supply. Relatively uniform illumination of round skin spots (diameter, 18 mm) is achieved using an advanced optical design that also reduces laser speckle artifacts [26].

A detailed description of the different smartphone-based multi-laser illumination prototypes and their validation can be found in Refs. [20,27].

2.2 Prototype device for skin fluorescence imaging using a smartphone

If light is absorbed in skin, it can be further re-emitted at longer wavelengths in the process of autofluorescence, i.e.,

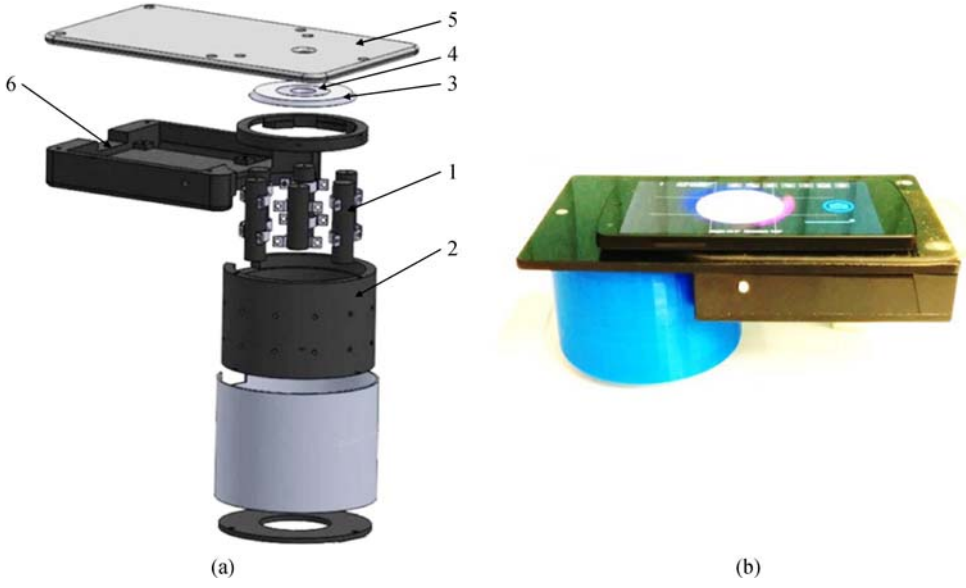

Fig. 6 Design scheme of the three-wavelength laser add-on illuminator (a) and the mobile prototype with a smartphone on it (b). 1 – laser modules (three pairs; 448, 532, and 659 nm), 2 – shielding cylinder, 3 – laser beam collector, 4 – flat ring-shaped diffuser of laser light, 5 – sticky platform for the smartphone, 6 – electronics compartment

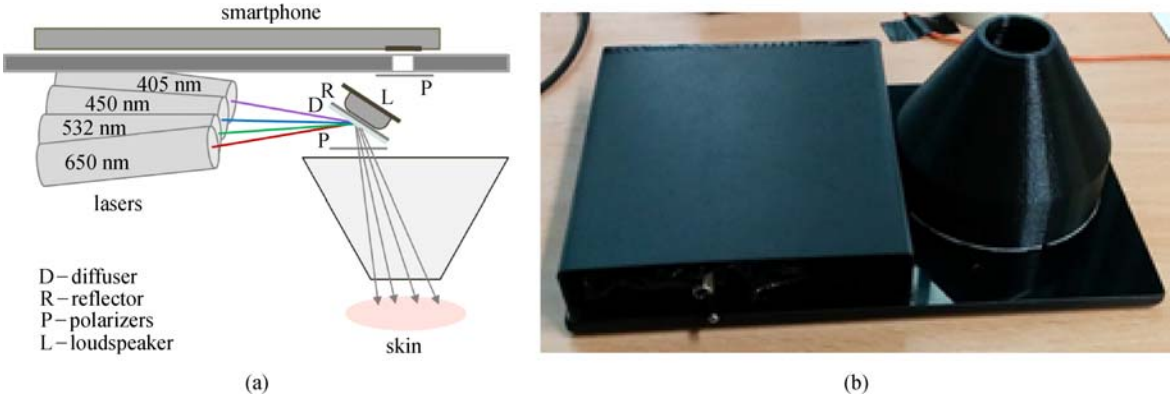

Fig. 7 Design scheme (a) and outlook (b) of the prototype device for switchable four-laser-wavelengths skin illumination

self-fluorescence without any specific additives on or inside the skin. The upper layers of skin house some fluorescing compounds, called fluorophores, each having a characteristic emission spectrum. Even if excited by a narrow laser line, several emission spectra overlap and the skin autofluorescence spectrum usually is bell-shaped, without a pronounced structure. Besides, a phenomenon called autofluorescence photobleaching (AFPB) normally takes place: the skin-emitted intensity decreases during continuous optical excitation and does not fully recover after even after such excitation is interrupted (Fig. 8). AFPB is responsible for some interesting effects, such as light-induced "fingerprints" on *in vivo* skin [28].

The reduction in the skin autofluorescence intensity during irradiation by lasers in most cases can be approximated by a double-exponential function:

$$I(t) = a\exp(-t/\tau_1) + b\exp(-t/\tau_2) + A, \qquad (1)$$

where I is the autofluorescence intensity for a fixed wavelength band, t is time, a and b are weighting coefficients, A is the "bottomline" constant, and τ_1, τ_2 are the fast and slow AFPB rate coefficients, respectively. The "fast" AFPB (when a sharp reduction in intensity is observed) usually takes place during the first 5–15 s of irradiation, while the "slow" AFPB continues up to several minutes.

Our first setup for skin AFPB imaging was based on a consumer photo-camera equipped with a band-pass filter in front of the objective; it was operating in a slow video mode (~2 frames/s) [31]. After image processing, the distribution of τ values over the imaged skin area was mapped and analyzed. This study showed that the τ values are sensitive to the skin structural changes; e.g., AFPB rates detected from melanin-pigmented nevi were always slower than those detected from healthy skin. Thus, AFPB rate measurements and spatial mapping may be useful for skin diagnostics and recovery monitoring, as well as for better delineation of skin tumor margins.

As a next step, a smartphone-compatible technique for acquisition and analysis of violet LED excited skin fluorescence intensity and AFPB rate distribution images has been developed and clinically tested. The design of the prototype device is shown in Fig. 9. For parametric mapping of the reduction rate in the skin AF intensity, a sequence of AF images under continuous 405-nm-wavelength LED (model LED Engin LZ1-00UA00-U8;

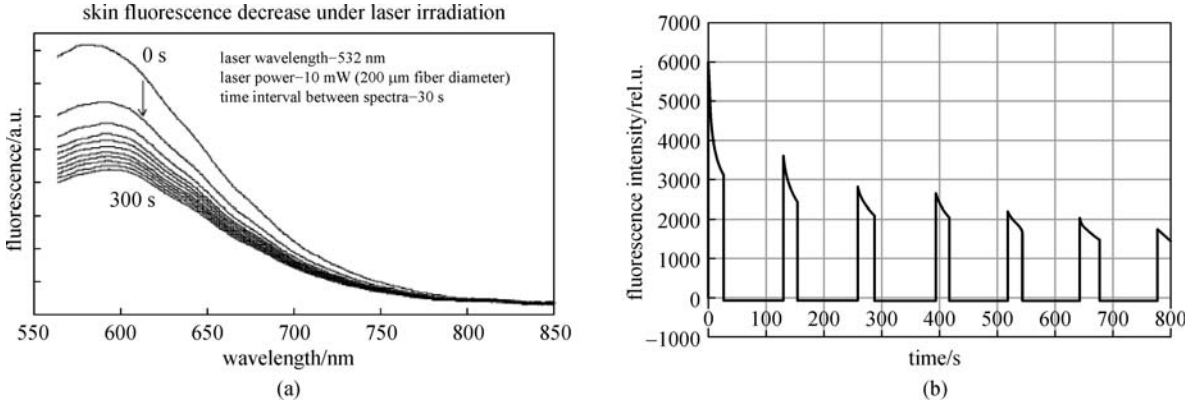

Fig. 8 Skin autofluorescence photobleaching under continuous 532-nm-wavelength laser irradiation (10–85 mW/cm^2). (a) Temporal changes in the emission spectrum [29]; (b) partial recovery of the autofluorescence intensity after interrupted excitation [30]

spectral band half-width, 30 nm) excitation for 20 s at a power density of ~20 mW/cm^2 with a framerate of 0.5 fr/s was recorded and analyzed. Four battery-powered violet LEDs placed within a cylindrical light-shielding wall (which also ensured a fixed 60 mm distance between the smartphone's camera and skin) evenly irradiated a 40-mm-radius round spot of the examined skin tissue. A long pass filter ($>$ 515 nm) was placed in front of the smartphone's camera to prevent detection of the exciting LED emission. The battery/electronics compartment comprised a set of rechargeable batteries and a *Bluetooth Low Energy* (BLE) module with a driver for communications between the smartphone and illumination unit. The recorded RGB fluorescence images were further separated to exploit the R- and G-images for imaging of skin autofluorescence in the red and green spectral bands, respectively. Due to a spectral cutoff by the 515-nm-wavelength long pass filter, the B band images served only for reference. The *Samsung Galaxy Note 3* smartphone, comprising an integrated CMOS RGB image sensor with the resolution of 13 MP, was used for image acquisition. All images were acquired with the following settings: ISO–100, white balance — daylight, focus — manual, exposure time – fixed 200 ms.

A detailed description of the design of this prototype and its clinical testing is provided in Ref. [32].

2.3 Photoplethysmography video-imaging prototypes

The incident cw light can be reflected from the skin surface and also may enter its epidermal and dermal layers where light can be absorbed and/or scattered. Some back-scattered photons travel via the skin dermal layer where arterial blood volume periodically changes with each heartbeat. As a consequence, total blood absorption also changes with each heartbeat and the intensity of the back-scattered light is modulated – the detected so-called remission photoplethysmography (PPG) signal comprises a relatively stable DC component, determined by the absorption characteristics of "static" skin structures, and a pulsatile AC component owing to the periodically changing blood absorption [33]. The pulsatile remission PPG signals can be detected not only using specially designed skin contact probes [34], but also remotely, e.g., by video-imaging of skin with subsequent signal processing [35]. This technique is called PPG-imaging (PPGI) or remote PPG (rPPG). The captured video signals consist of a number of image frames taken at a definite frame rate, e. g., 20 frames/s. Consequently, during one cycle of heart activity (~1 s) 20 skin images are acquired, each for a different phase of the sub-cutaneous pulse wave. If consecutive frames are compared, the skin-remitted light intensity detected from a fixed area increases and decreases with time, forming the periodic PPGI signal. Specific software [36] allows to extract arterial pulsations from video signals over the entire imaged skin area. The amplitudes of PPG peaks may differ across the image pixels owing to differences in blood perfusion characteristics of different skin tissues – especially if there is a burn or other type of dermal skin damage. After image processing, parametric maps of the PPG signal amplitude distribution (or blood perfusion maps) can be constructed [37].

Figure 10 illustrates the recently designed PPGI prototype device for distant monitoring of anesthesia efficiency during the palm surgery. The system was designed to record signals from the curved surface of the hand (dorsal or ventral aspect). The illuminator comprised four bispectral light sources, each consisting of two high-power LED emitters (Roithner LaserTechnik *GmbH*; green: λ = 530 nm, 3 W; IR: λ = 810 nm, 1 W). To achieve uniform illumination of the skin surface, an adjustable LED intensity control was introduced via PC based custom developed software. The two wavelengths of illumination were chosen in order to control blood pulsations at two different vascular depths in real time [38]. A microcontroller board (Arduino Nano, Arduino,

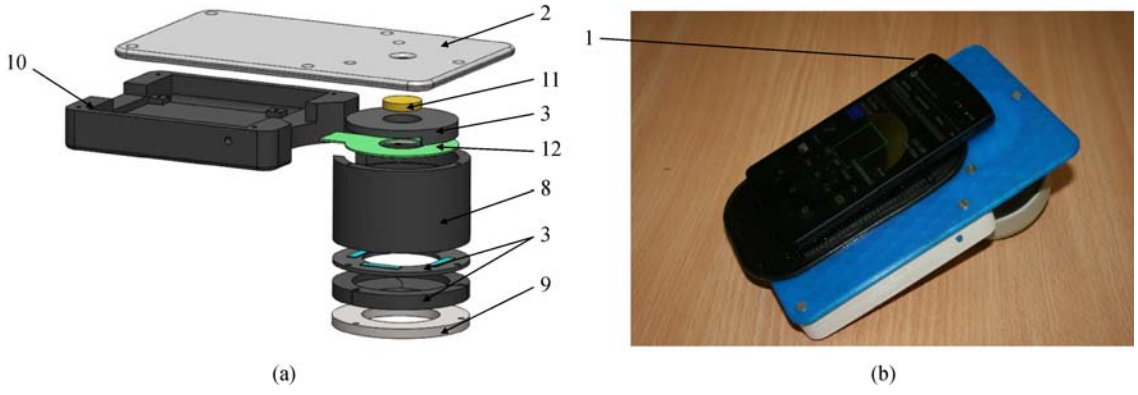

Fig. 9 Design scheme (a) and outlook (b) of the prototype device for skin fluorescence imaging using a smartphone. 1 – smartphone, 2 – sticky fixing plate with camera window, 3 – mounting rings, 8 – cylindrical screening spacer, 9 – silicone skin-contact ring, 10 – battery/electronics compartment, 11 – long-pass filter, 12 – LED ring

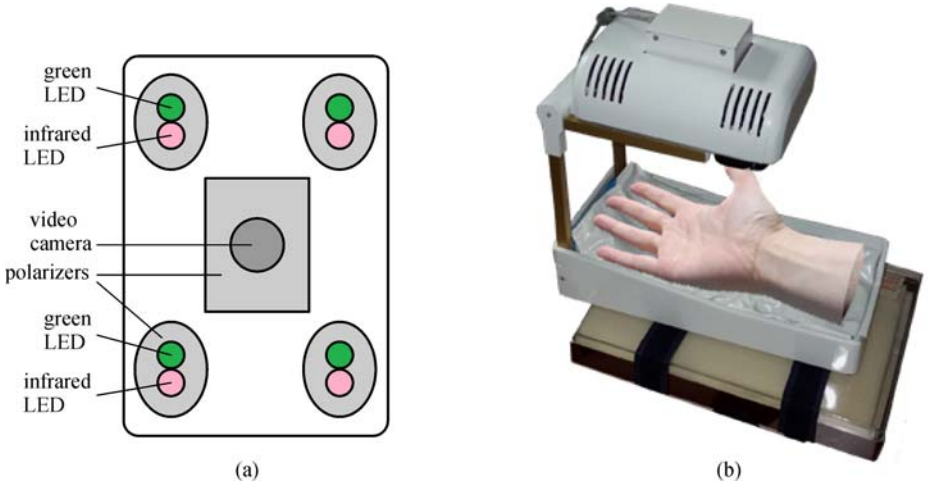

Fig. 10 Hardware components of the dual-wavelength photoplethysmography imaging device. The bottom view of the imaging system-camera and light sources (a), and the entire device with a vacuum pillow supporting the palm (b)

USA) provided sequential switching of green and IR LEDs and triggering of the captured video frames. The camera control was performed using *uEye* software in the manual trigger mode, with fixed exposure time, 2 × 2 pixel binning and triggered at 60 frames/s. A monochromatic camera (8 bit CMOS *IDS-uEye UI-1221LE*) was equipped with *S-mount* 1/2 inch $F = 4$ mm low distortion, wide-field lens (Lensagon). The camera lens was placed at the distance of 15 cm from the skin surface, to ensure a full view of the adult palm (field of view, 20 cm × 15 cm). To reduce the skin specular reflectance, orthogonally oriented polarizers were placed behind the camera and all four light sources, respectively. The plastic parts were fabricated using a 3D printer (Prusa i3, custom made, Latvia). The device comprised a plastic enclosure filled with an adjustable vacuum pillow (40 × 20 AB Germa, Sweden) as the palm support.

Another, much smaller PPGI prototype device (Fig. 11) was developed for distant monitoring of skin microcirculation during various surgeries. This device comprised a near-IR LED illuminator and a video camera, both placed in a custom designed 3D-printed case (4 cm × 4 cm × 4 cm). The illuminator comprised a ring of 12 circularly oriented near-IR LEDs (peak wavelength, 760 nm; current, 20 mA each), connected in parallel; stabilized illumination was provided by a LED driver (cat4104). Video acquisition was performed using a board-level CMOS video camera (*IDS uEye UI-1221LE*), maximal resolution of 752 × 480 pixels, maximal framerate of 87 frames/s, 8-bit monochrome). The camera was equipped with a low-distortion S-mount 4-mm-diameter lens (*Lensagon*). To reduce the skin specular reflectance, cross-oriented polarizers were placed behind the light sources and in front of the camera, respectively. An IR cutoff filter KC-15 (> 700 nm) was also placed in front of the camera, to minimize the influence of ambient illumination. The device was

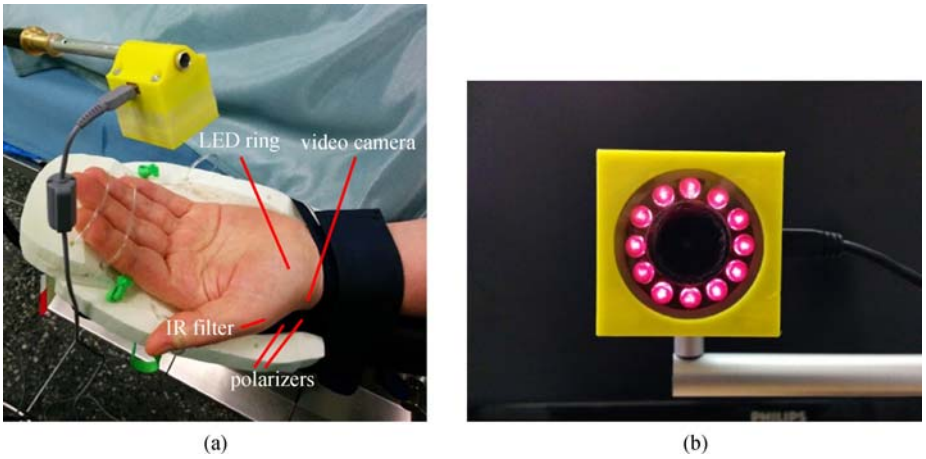

Fig. 11 Compact PPGI prototype device in operation (a) and the front view of the device (b)

connected via an USB-2 cable to a PC, which also served for power supply.

A detailed description of the developed PPGI prototype devices and their software can be found in Refs. [36,37,39].

2.4 Multimodal skin imagers

2.4.1 *SkImager* – a concept device

A proof-of-concept prototype device, utilizing inexpensive components and smart software, was developed for more advanced, compact, and handy wireless skin diagnostics and monitoring. Multimodal imaging amounts to capturing a number of spectral and video images from the skin area affected by pathology, with subsequent extraction of clinically significant information. The device performs four imaging tasks in series, collecting: 1) an RGB image of skin under illumination by a white polarized LED, which helps to reveal hidden subcutaneous structures; 2) four spectral images under narrowband LED illumination for mapping the main skin chromophores; 3) video images under green LED illumination for mapping blood perfusion in the analyzed skin; 4) video images of autofluorescence under UV LED irradiation for mapping the skin fluorophores. Polarized LED light is used for illumination, and round skin spots (diameter, 34 mm) are imaged by a CMOS sensor via a cross-oriented polarizing filter. To improve the reliability of diagnostics, manipulation with maps of different parameters (i.e., extraction, summing, and division of images) is proposed as well. The first prototype version was described earlier [40].

Design details of an advanced prototype device with preliminary brand-name "*SkImager*" (Fig. 12) are discussed below. It is a battery-powered fully wireless device. Its main building blocks are a CMOS image sensor, a LED illumination system, an on-chip microcomputer, a touchscreen, a memory unit, and a rechargeable battery. The functional diagram of the device is presented in Fig. 12(c). A system on chip (SoC) module *Nvidia Tegra 2 T20* with a dual-core *ARM Cortex-A9* processor (clock frequency, 1 GHz) is used as a central processing unit. It provides smooth operation of all the device's components. A 3 Mpix RGB CMOS matrix with 3.2-μm-size pixels (MT9T031) serves as the image sensor; it is connected to a central processor via a 10-bit parallel line. A removable SD memory card stores the image information that can be transferred to an external processor, e.g., a PC. This can also be accomplished using a Mini-USB connector, which also enables installing and updating the software. Thus, on-board and off-board calculations can be performed for extracting parametric maps of the examined skin area. The main information input-output device is the built-in 4.3 inch/480 × 272 pixel touchscreen. It displays the operation mode and state of the device (battery charge level, clock, state of the memory card). A power switch button is placed on the side above the slot of the memory card (Fig. 12(b)).

The device has a holder with integrated contacts for battery charging (Fig. 12(a)). A Li-ion battery (3.6 V, 4.6 Ah) ensures up to 15 h of operation, providing about 100 full measurement cycles. The power consumption under the maximal load (display switched-on, spectral and video image recording and processing) is 3 W, or 1 W in the waiting mode. The dimensions of the device are 121 mm × 205 mm × 101 mm, and its mass is ~440 g. The specific skin illumination is accomplished by a ring of LEDs surrounding the objective of a CMOS (Aptina) image sensor (Fig. 12(b)). In total, 24 LEDs are operated – sets of 4 diodes emitting at five various wavelength bands (peaks at 365, 450, 540, 660, and 940 nm – Fig. 13(a)), and 4 white LEDs. Each set of equal LEDs is powered separately by a 6-channel LED driver (Fig. 12(c)), in order to provide the same illumination intensity and constant signal output by the visible and near IR diodes. A three-color RGB CMOS sensor has the resolution of 2048 × 1536 pixels with the maximal acquisition rate of 25 frames/s. The spectral sensitivity bands of the CMOS sensor are shown in Fig. 13(b). To minimize the detection of surface-

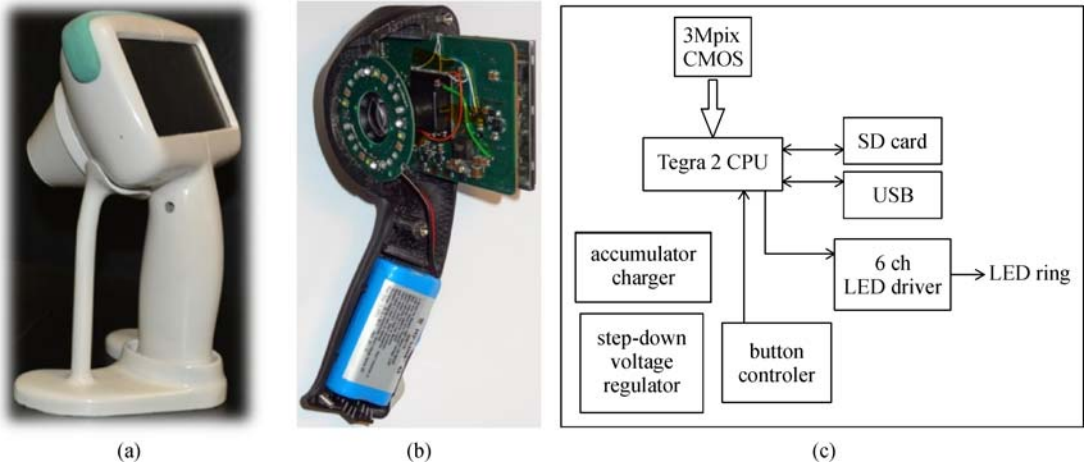

Fig. 12 *SkImager* prototype device in its battery-charging holder (a), internal design details (b) and functional scheme (c)

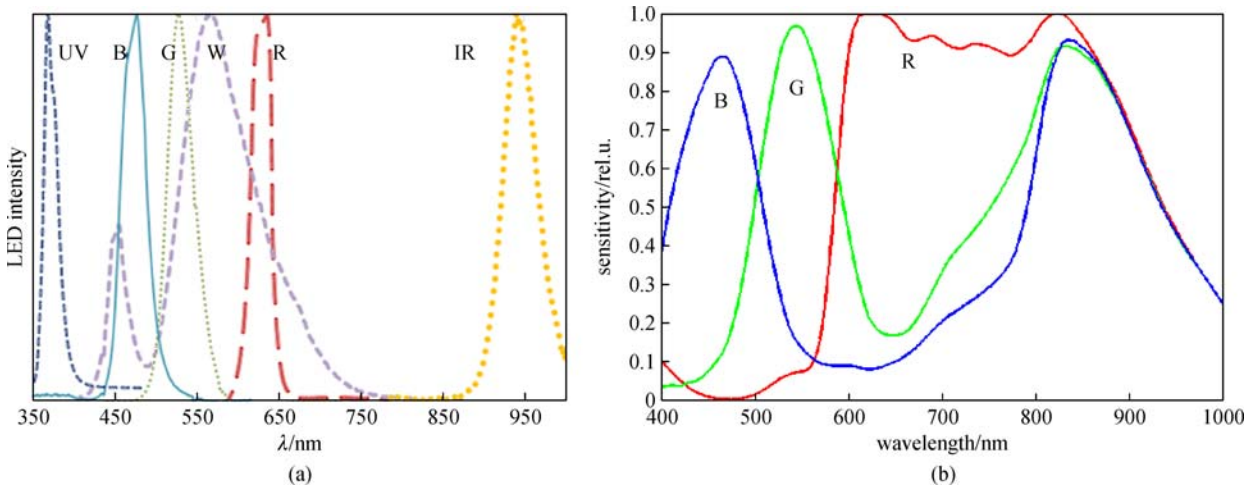

Fig. 13 Measured emission bands of exploited LEDs (a) and spectral sensitivities of the CMOS image sensor (b)

reflected light, crossed film polarizers cover the LED ring and the camera's objective (S-Mount M12x0.5), respectively. To maintain the distance to the skin at 55 mm, two easily changeable conical tips are used, with the target field diameters 34 and 11 mm. The latter is intended for skin imaging of curved surfaces, such as the nose. The internal surfaces of the tips are black-coated and multiple-step shaped to suppress any side-reflected light.

A detailed description of the *SkImager* prototype and its validation is provided in Ref. [41].

2.4.2 Modular multimodal skin imager

Another prototype for multimodal skin imaging has been designed as a 3D-printed modular device that comprises three main modules (Fig. 14):

1) Processing, wireless transmission and power block;
2) Camera and lens block;
3) Illumination block.

The first (processing and communication) module uses an embedded computer, Raspberry Pi [42], as its main processing unit. Wireless connections are realized by WiPi USB dongles, and a rechargeable battery is used as the power source. Charging is performed by connecting a USB cable, similar to the charging of mobile phones. All elements use standard interfaces and can be replaced just by plugging a cable into the new device.

The second (imaging) module holds an "IDS uEye UI-3581LE-C-HQ" camera [43] and a "Lensagon BVM8020014" lens. The camera uses the USB interface and allows upgrading to a new camera without any changes in hardware and software. The camera was chosen to be IDS, because this manufacturer provides a wide range of cameras and all of them share the same physical and software design. By using two lens mounts ("C type" and "S type") lenses can be interchanged easily.

The third (illumination) module ensures three imaging modes: multispectral imaging of diffuse reflectance (spectral bands with maxima at 435, 535, 660, 740, and 940 nm), fluorescence spectral imaging (excitation at 405 nm), and 635-nm-wavelength laser speckle imaging. A custom printed board was created for managing skin

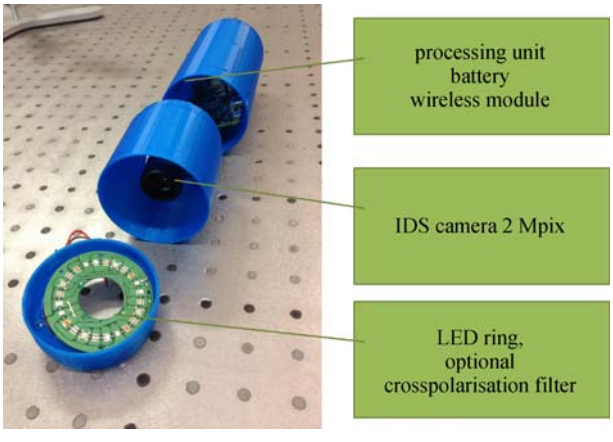

Fig. 14 Photograph of the 3D-printed modular multimodal imaging prototype device

illumination by narrowband LEDs. It uses a standard interface for selecting the current illumination band; therefore, changing the light source requires less effort than with fully customized existing designs.

By using his/her own smartphone or laptop, the user connects to the device's WiFi network and controls the process of imaging via a browser. During the first step, the user should use the operating system's procedure for connecting to the WiFi network (the WiFi network is password-protected). In the second step, the user selects whether he/she requires a new image capture or wishes to view previously captured images. In the third step, the user targets the skin region to be captured by viewing a live video stream from the camera. Images are captured by pressing a physical button located on the device. The capturing process can be repeated. After the image acquisition, the user can switch to the last step – viewing the results. A typical time delay between the completion of image acquisition and viewing the results is less than 10 s.

A more detailed description of this device and its validation is presented in Refs. [44,45].

3 Summary and conclusions

Designs of nine laboratory-made prototype devices for diagnostic skin imaging have been discussed:

1) An RGB-LED system for smartphone multispectral imaging;

2) A modified video microscope for multispectral imaging;

3) A three-wavelengths smartphone illuminator for monochromatic spectral imaging;

4) A four-wavelengths smartphone illuminator for monochromatic spectral imaging;

5) A smartphone-based skin fluorescence imager;

6) A photoplethysmography imager for palm surgeries;

7) A compact (4 cm × 4 cm × 4 cm) photoplethysmography imager;

8) *SkImager* – a multimodal skin imaging concept device;

9) A modular multimodal skin imager.

The operational principles and design details of the hardware were emphasized in this review, with less attention paid to the developed software and the laboratory and clinical tests of the prototypes. Information on the latter is available in our papers cited at the ends of subchapters.

In general, all of the considered prototypes demonstrated adequate functionality, thus confirming the viability of the applied design concepts. On the other hand, the measurements that were performed in real clinical settings showed that there is still room for optimization of the designs and for improvements of the software, to make it more user-friendly and to provide better sensitivity and specificity of clinically significant parameters. Research in these directions is ongoing, as are attempts to commercialize the most successful prototypes.

Acknowledgements The above presented prototypes were created in teamwork, so author first would thank the current and previous laboratory colleagues for the significant contributions- see their names in the reference list. The financial support by European Regional Development Fund and by Latvian national research program SOPHIS under the grant agreement #10-4/VPP-4/11 is highly appreciated.

References

1. Spigulis J. Biophotonic technologies for noninvasive assessment of skin condition and blood microcirculation. Latvian Journal of Physics and Technical Sciences 2012, 49(5): 63–80
2. http://www.imaging.org/site/PDFS/Reporter/Articles/REP27_4_CIC20_TOMINAGA_p177.pdf (accessed on 12.03.2017)
3. Jakovels D, Spigulis J, Rogule L. RGB mapping of hemoglobin distribution in skin. Proceedings of the Society for Photo-Instrumentation Engineers, 2011, 8087: 80872B
4. Jakovels D, Kuzmina I, Berzina A, Valeine L, Spigulis J. Noncontact monitoring of vascular lesion phototherapy efficiency by RGB multispectral imaging. Journal of Biomedical Optics, 2013, 18(12): 126019
5. Jakovels D, Spigulis J. 2-D mapping of skin chromophores in the spectral range 500 – 700 nm. Journal of Biophotonics, 2010, 3(3): 125–129
6. Jakovels D, Spigulis J. RGB imaging device for mapping and monitoring of hemoglobin distribution in skin. Lithuanian Journal of Physics, 2012, 52(1): 50–54
7. Philips Vital Signs Camera. http://www.vitalsignscamera.com/ (accessed on 12.03.2017)
8. The best heart disease iPhone & Android Apps of the year. http://www.healthline.com/health-slideshow/top-heart-disease-iphone-android-apps#5 (accessed on 12.03.2017)
9. Skinvision. https://www.skinvision.com/technology-skin-cancer-melanoma-mobile-app (accessed on 12.03.2017)
10. Spigulis J, Lacis M, Kuzmina I, Lihacovs A, Upmalis V, Rupenheits Z. Method and device for smartphone mapping of tissue compounds. WO 2017/012675 A1, 2017
11. Kuzmina I, Lacis M, Spigulis J, Berzina A, Valeine L. Study of smartphone suitability for mapping of skin chromophores. Journal of Biomedical Optics, 2015, 20(9): 090503
12. http://www.dino-lite.com/applications_list.php?index_id = 8 (accessed on 12.03.2017)
13. http://www.dino-lite.com/products_detail.php?index_m1_id = 0&index_m2_id = 0&index_id = 61 (accessed on 12.03.2017)
14. Diebele I, Kuzmina I, Lihachev A, Kapostinsh J, Derjabo A, Valeine L, Spigulis J. Clinical evaluation of melanomas and common nevi by spectral imaging. Biomedical Optics Express, 2012, 3(3): 467–472
15. Bekina A, Diebele I, Rubins U, Zaharans J, Derjabo A, Spigulis J. Multispectral assessment of skin malformations by modified video-microscope. Latvian Journal of Physics and Technical Sciences, 2012, 49(5): 4–8
16. Bekina A, Rubins U, Lihacova I, Zaharans J, Spigulis J. Skin

chromophore mapping by means of a modified video-microscope for skin malformation diagnosis. Proceedings of the Society for Photo-Instrumentation Engineers, 2013, 8856: 88562G
17. Rubins U, Zaharans J, Lihacova I, Spigulis J. Multispectral video-microscope modified for skin diagnostics. Latvian Journal of Physics and Technical Sciences, 2014, 51(5): 65–70
18. Spigulis J, Elste L. Method and device for imaging of spectral reflectance at several wavelength bands. WO2013135311 (A1), 2012
19. Spigulis J, Jakovels D, Rubins U. Multi-spectral skin imaging by a consumer photo-camera. Proceedings of the Society for Photo-Instrumentation Engineers, 2010, 7557: 75570M
20. Spigulis J, Oshina I. Snapshot RGB mapping of skin melanin and hemoglobin. Journal of Biomedical Optics, 2015, 20(5): 050503
21. Spigulis J, Oshina I, Berzina A, Bykov A. Smartphone snapshot mapping of skin chromophores under triple-wavelength laser illumination. Journal of Biomedical Optics, 2017, 22(9): 091508
22. Prahl S. Tabulated molar extinction coefficient for hemoglobin in water. http://omlc.ogi.edu/spectra/hemoglobin/summary.html (accessed 30 November 2016)
23. Sarna T, Swartz H M. The physical properties of melanin. http://omlc.ogi.edu/spectra/melanin/eumelanin.html (accessed 30 November 2016)
24. Spigulis J, Elste L. Single-snapshot RGB multispectral imaging at fixed wavelengths: proof of concept. Proceedings of the Society for Photo-Instrumentation Engineers, 2014, 8937: 89370L
25. Spigulis J, Oshina I. Method and device for chromophore mapping under illumination by several spectral lines. LV patent 15106 B, 2016
26. Rubins U, Kviesis-Kipge E, Spigulis J. Device for obtaining speckle-free images at illumination by scattered laser beams. LV patent application P-17–17, 2017
27. Oshina I, Spigulis J, Rubins U, Kviesis-Kipge E, Lauberts K. Express RGB mapping of three to five skin chromophores. OSA Technical Digests, 2017 (ECBO Proceedings, Munich, in press)
28. Lihachev A, Lesins Jh D, Jakovels J, Spigulis. Low power cw-laser signatures on human skin. Quantum Electronics, 2011, 40(12): 1077–1080
29. Stratonnikov A A, Polikarpov V S, Loschenov V B. Photobleaching of endogenous fluorochroms in tissues *in vivo* during laser irradiation. Proceedings of the Society for Photo-Instrumentation Engineers, 2001, 4241: 13–24
30. Lesinsh J, Lihachev A, Rudys R, Bagdonas S, Spigulis J. Skin autofluorescence photobleaching and photo-memory. Proceedings of the Society for Photo-Instrumentation Engineers, 2011, 8092: 80920N
31. Spigulis J, Lihachev A, Erts R. Imaging of laser-excited tissue autofluorescence bleaching rates. Applied Optics, 2009, 48(10): D163–D168
32. Lihachev A, Derjabo A, Ferulova I, Lange M, Lihacova I, Spigulis J. Autofluorescence imaging of basal cell carcinoma by smartphone RGB camera. Journal of Biomedical Optics, 2015, 20(12): 120502
33. Allen J. Photoplethysmography and its application in clinical physiological measurement. Physiological Measurement, 2007, 28 (3): R1–R39
34. Spigulis J. Optical noninvasive monitoring of skin blood pulsations. Applied Optics, 2005, 44(10): 1850–1857
35. Rubins U, Upmalis V, Rubenis O, Jakovels D, Spigulis J. Real-time photoplethysmography imaging system. Proceedings of IFMBE, 2011, 34: 183–186
36. Rubins U, Spigulis J, Miscuks A. Photoplethysmography imaging algorithm for continuous monitoring of regional anesthesia. In: Proceedings of the 14th ACM/IEEE Symposium on Embedded Systems for Real-Time Multimedia, ESTIMedia'16. 2016: 67–71
37. Rubins U, Spigulis J, Miscuks A. Application of color magnification technique for revealing skin microcircuration changes under regional anaesthetic input. Proceedings of the Society for Photo-Instrumentation Engineers, 2013, 9032: 903203
38. Spigulis J, Gailite L, Lihachev A, Erts R. Simultaneous recording of skin blood pulsations at different vascular depths by multi-wavelength photoplethysmography. Applied Optics, 2007, 46(10): 1754–1759
39. Marcinkevics Z, Rubins U, Zaharans J, Miscuks A, Urtane E, Ozolina-Moll L. Imaging photoplethysmography for clinical assessment of cutaneous microcirculation at two different depths. Journal of Biomedical Optics, 2016, 21(3): 035005
40. Spigulis J, Garancis V, Rubins U, Zaharans E, Zaharans J, Elste L. A device for multimodal imaging of skin. Proceedings of the Society for Photo-Instrumentation Engineers, 2013, 8574: 85740J
41. Spigulis J, Rubins U, Kviesis-Kipge E, Rubenis O. SkImager: a concept device for *in-vivo* skin assessment by multimodal imaging. Proceedings of the Estonian Academy of Sciences, 2014, 63(3): 213–220
42. Embedded linux on board computer decsription, https://www.raspberrypi.org/ (accessed on 12.03.2017)
43. Industrial USB cameras description, https://en.ids-imaging.com/ (accessed on 12.03.2017)
44. Bliznuks D, Jakovels D, Saknite I, Spigulis J. Mobile platform for online processing of multimodal skin optical images: using online Matlab server for processing remission, fluorescence and laser speckle images, obtained by using novel handheld device. In: Proceedings of BioPhotonics 2015 (Florence). 2015: 7304024
45. Jakovels D, Saknite I, Bliznuks D, Spigulis J, Kadikis R. Benign-atypical nevi discrimination using diffuse reflectance and fluorescence multispectral imaging system. In: Proceedings of BioPhotonics 2015 (Florence). 2015: 7304026

Janis Spigulis graduated as physicist from the University of Latvia in 1973. Later, he obtained his Ph.D. degree in optics (1979) and Dr. Habil. Phys. degree in technical physics (1993). Currently, he is the head of the Biophotonics Laboratory at the Institute of Atomic Physics and Spectroscopy and a professor at the Physics Department, University of Latvia. He has been teaching and doing research on biomedical optics and biophotonics since 1995, mainly focusing on non-invasive and non-contact optical diagnostics and monitoring techniques.

More details: http://home.lu.lv/~spigulis.